Research Article

Journal of Environmental Nanotechnology

Metal–organic Frameworks for Sustainable Water Disinfection: Synthesis, Characterization and Antimicrobial Properties

Suman Thakur and Sharda Bharti*

Department of Biotechnology, National Institute of Technology (NIT) Raipur, Raipur, CG, India

Received: 04.05.2024 Accepted: 19.06.2024 Published: 30.06.2024

*sbharti.bt@nitrr.ac.in

ABSTRACT

Waterborne biological pollution poses a significant threat to both the environment and human health, leading to the transmission of various waterborne diseases. Ensuring the safety of drinking water is essential for safeguarding public health and reducing the prevalence of waterborne illnesses caused by microbial pollutants. Recently, there has been a notable increase in the utilization of nanoparticles for water treatment purposes. Metal-Organic Frameworks (MOFs) are emerging as promising candidates for enhancing water treatment processes due to their structural and functional adjustability, which makes them suitable for environmental remediation. Notable properties include porous structures with customizable sizes, large surface areas, and internal characteristics that are variable. In this study, zeolitic-imidazolate frameworks (ZIF-8) and Ag@zeolitic-imidazolate frameworks (Ag@ZIF-8) were synthesized using 2-methylimidazole (2-MIM) as an organic linker *via* a facile green synthesis method and were used for water disinfection. The MOFs were characterized using a range of techniques, including UV-Vis spectroscopy, FTIR, X-ray diffraction, and SEM/EDS. The antibacterial activity of ZIF-8 and Ag@ZIF-8 was evaluated using the disc diffusion method against Gram-negative and Gram-positive bacteria, i.e., *E. coli* and *S. aureus*, respectively. Strong antimicrobial activity was demonstrated against both Gram-positive and Gram-negative bacteria with Ag-ZIF-8 MOF exhibiting improved antibacterial activity over ZIF-8 alone. The proposed material shows promise for reusable water filtration and disinfection against a variety of pollutants, providing a practical option to reduce environmental and public health threats.

Keywords: Antimicrobial properties; Environmental remediation; Metal-organic frameworks; Water disinfection; Zeolitic-imidazolate frameworks.

1. INTRODUCTION

Waterborne biological pollution is a serious hazard to both the environment and human health since it may cause the spread of a variety of waterborne illnesses. Biological contamination of drinking water refers to microorganisms such as bacteria, viruses, fungi, protozoa, and helminths in water sources suitable for human use (Kumar *et al.* 2022). Metal-organic frameworks (MOFs) might be employed as antibacterial agents as well as water treatment materials. Metal ions or clusters interact with organic ligands to form MOFs. Over the last two decades, there have been significant advances in MOF research in the field of solid-state chemistry (Amargeetha *et al.* 2018). Metal-organic frameworks are particularly desirable porous materials due to their outstanding features, such as their high specific surface area, extraordinary thermal and chemical durability across a broad variety of conditions, and the flexibility to modify pore sizes (Thakur *et al.* 2023). The extensive use of MOFs in many industries is attributed to these exceptional advantages. Recent studies indicate that MOFs are highly regarded as potential supports for metal nanoparticles and are considered superior to other porous materials such as clay, zeolites, and silica in a wide range of applications (Gu *et al.* 2020). Zeolitic imidazolate frameworks, often known as ZIFs, have shown substantial development in recent years. The structures of these compounds are based on tetrahedral units, where each metal ion (M) (such as Zn or Co) is bound to four organic imidazolate (Im) linkers (M−Im−M). Zeolitic Imidazolate Frameworks are considered a subset of MOFs, and traditionally, their structure has closely matched that of zeolites (Shahsavari *et al.* 2022). ZIFs possess the desirable attributes of both MOFs and zeolites, such as porosity, crystallinity, and remarkable chemical and thermal stability. They exhibit a diameter and pore width of 3.4 Å and 11.6 Å, respectively. The structure of ZIF-8 ($Zn(mIm)_2$), in which mIm is 2-methyl imidazolate, is characterized by a solidate architecture, and it possesses a space group consisting of linked six-membered ring windows (Bergaoui *et al.* 2021). ZIF-8 is the most well-known and established member of the ZIF family, and as a result, a significant amount of research is being conducted on its unique characteristics. Furthermore, ZIFs are considered attractive choices for several purposes such as sensing, catalysis, adsorption, membrane gas separation, and

antimicrobial applications (Salehipour *et al.* 2021). One of the advantages of ZIF-8 nanoparticles is that their extraordinary stability makes it possible for them to be used for extended periods (Yuan *et al.* 2017).

MOFs are suitable materials for incorporating silver nanoparticles (AgNPs), and the presence of Zn^{2+} cations in the ZIF-8 structure enhances the antibacterial activity of silver ions through a synergistic effect (Abdi, 2020). Silver nanoparticles have attracted significant attention for their potential as antimicrobial agents in combating bacterial infections. Due to their distinctive characteristics, such as a high surface-area-to-volume ratio and potent antibacterial capabilities, they are considered very promising for a range of applications, including antimicrobial (Bharti *et al.* 2019; Bharti *et al.* 2020; Bharti *et al.* 2021) and biomedical/therapeutic applications (Bharti *et al.* 2023b; Bharti *et al.* 2023a; Bharti *et al.* 2024). This antimicrobial action is achieved by disrupting the cell membrane, entering the microorganism, and harming the cell. It was discovered that AgNPs had a significantly lower effect on the Gram-positive bacteria because of the structural differences in cell wall composition between Gram-positive and Gram-negative bacteria. Gram-negative bacteria possess an outer coating of lipopolysaccharides, which is situated beneath a thin layer of peptidoglycan measuring 7–8 nm in thickness. In contrast, the cell wall of Gram-positive bacteria mostly consists of a substantial layer (20–80 nm) of peptidoglycan. This peptidoglycan is made up of linear polysaccharidic chains that are crosslinked by short peptides, resulting in a solid three-dimensional structure. The rigidity and widespread formation of chemical bonds not only decrease the locations on the bacterial cell wall where AgNPs may attach, but also make it more challenging for the particles to enter the wall (Franci *et al.* 2015). The incorporation of MOFs with inorganic compounds can significantly enhance the antibacterial efficacy of the complexes. The bacterial inhibitory activity was improved by combining ZIF-8 with Ag in this experiment. ZIF-8, due to the presence of the Zn^{2+} core metal ion, has antibacterial properties and can be utilized as an antibacterial agent (Bao *et al.* 2023). Guo et al. effectively produced core-shell Ag@ZIF-8 nanowires, which exhibited notable antibacterial properties against *E. coli* and *B. subtilis* (Guo *et al.* 2018). Malik and colleagues produced multifunctional CdSNPs@ZIF-8 nanoparticles that exhibit antibacterial properties against both *E. coli* and *S. aureus* (Malik *et al.* 2018).

In this work, a straightforward and eco-friendly green synthesis technique was utilized to fabricate ZIF-8 and Ag@ZIF-8. Various analytical methods, including UV-Vis spectrophotometry, Fourier-transform infrared spectroscopy (FT-IR), X-ray diffraction (XRD), and scanning electron microscopy combined with energy-dispersive X-ray spectroscopy (SEM/EDS), were used to completely characterize the resulting nanomaterials. The antibacterial activity of the synthesized materials was then tested using the zone of inhibition (ZOI) test against both Gram-positive (*S. aureus*) and Gram-negative (*E. coli*) bacteria. ZIF-8 and Ag@ZIF-8 nanocomposites were both subjected to this analysis to examine the antibacterial properties. Overall, this research shows potential for creating new antimicrobial materials that might be used in several areas such as medicine, biotechnology, and environmental remediation. Further investigation in this area may help find solutions to the problems caused by antibiotic resistance and bacterial infections.

2. MATERIALS AND METHODS

2.1 Materials

The chemicals and reagents used include zinc nitrate hexahydrate ($Zn(NO_3)_2{\cdot}6H_2O$, ≥99.0%), silver nitrate ($AgNO_3$, ≥99.8%) acquired from Merck, 2-methylimidazole (Hmim, ≥99.0%), cobalt nitrate hexahydrate ($Co(NO_3)_2{\cdot}6H_2O$, ≥99.0%) purchased from Loba Chemie, India. Nutrient broth and bacteriological nutrient agar were purchased from HiMedia, India. Other chemicals i.e., ethanol, NaOH, HCl were of analytical grade, and were used as received. All chemicals in this research were used directly, without any additional purification. Furthermore, the antibacterial efficacy of the MOF and Ag-MOF was assessed using two bacterial strains, a Gram-negative bacterium, *Escherichia coli* and a Gram-positive bacterium, *Staphylococcus aureus* (MTCC 9542), which were obtained from the Institute of Microbial Technology (IMTECH, Chandigarh), India.

2.2 Methods

2.2.1 Synthesis of ZIF-8

ZIF-8 was synthesised in this work according to Abdi (2020) with slight modification. Fig. 1 illustrates the synthesis process of ZIF-8 nanoparticles. To prepare ZIF-8, a precursor solution comprising zinc cations ($Zn(NO_3)_2{\cdot}6H_2O$), H-MIM (2-methylimidazole) ligand, and deionized water was utilized. Initially, 1.487 g of $Zn(NO_3)_2{\cdot}6H_2O$ (0.05 M) was dissolved in deionized water. Simultaneously, 12.317 g of H-MIM (1.5 M) was dissolved in deionized water separately. The solution containing zinc nitrate was then slowly added dropwise to the solution containing the organic ligand. The resulting mixture was stirred using a magnetic stirrer for 2 hours at room temperature, maintaining a speed of 300 rpm, and adjusting the pH to 8. Subsequently, the milky white solution was centrifuged to separate the ZIF-8 particles. These particles were washed multiple times with ethanol and then with deionized water. Finally, the particles were dried overnight at 50 °C.

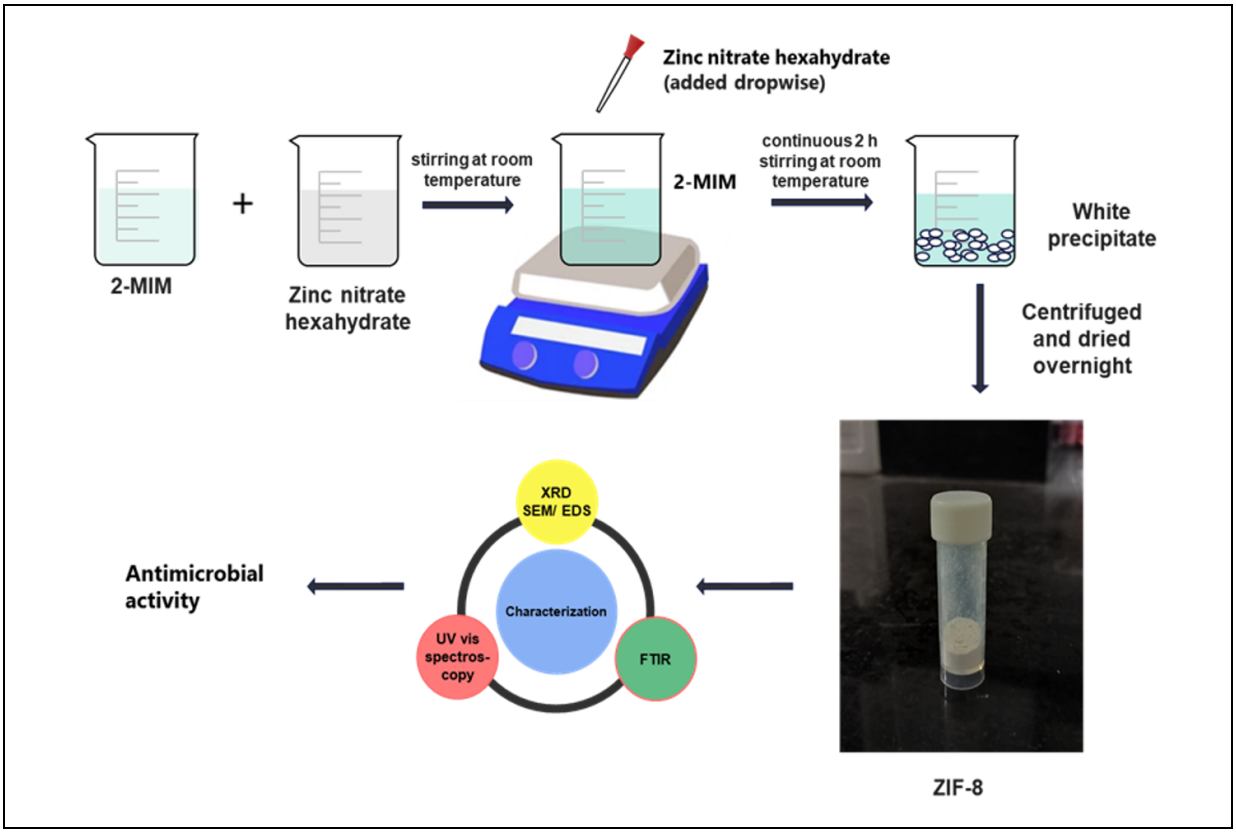


Fig. 1: Schematic representation of ZIF-8 synthesis

2.2.2 Synthesis of Ag@ZIF-8

The synthesis of Ag@ZIF-8 was conducted following the method described by Abdi (2020) with minor modifications. Initially, 0.125 g of $AgNO_3$ was introduced into a solution consisting of 20 mL of ethanol and deionized water. The resulting mixture was then agitated using a magnetic stirrer for 30 minutes at a speed of 300 rpm, at room temperature. Subsequently, 0.5 g of the synthesized ZIF-8 powder was evenly distributed throughout the mixture and stirred for two hours. The sample was designated as Ag@ZIF-8 nanocomposites. Subsequently, the Ag@ZIF-8 samples were separated using centrifugation, subjected to three rounds of ethanol washing to eliminate any remaining Ag^+ ions adsorbed onto the ZIF-8 MOF particles, and then dried at a temperature of 50 ℃ in an oven. The dried Ag@ZIF-8 nanocomposites were used for characterization and to assess their antimicrobial properties.

2.3 Characterization

The functional groups were characterized by detecting the molecular vibrations of the materials using Fourier transform infrared spectroscopy (Alpha II, Bruker). The materials were compressed into pellets, and the absorption range of 4500–500 cm^{-1} IR was recorded. UV-Vis spectra was recorded using double beam UV-Vis spectroscopy (1900i, Toshvin Analytical) in the range of 200–900 nm for the synthesized nanomaterials. The broad-angle X-ray diffraction of the ZIF-8 and Ag@ZIF-8 nanocomposites was measured over a scanning range of 10° to 80° using an X-ray diffractometer (PANalytical 3 kW X'pert Powder XRD – Multifunctional). Scanning Electron Microscopy was used to examine the surface morphologies of the material using ZEISS EVO Series Scanning Electron Microscope EVO 18.

2.4 Disc Diffusion Studies for Depicting Antibacterial Activity

The experiment utilized a newly obtained culture of Gram-positive *S. aureus* MTCC 9542 and Gram-negative *E. coli* K-12. Initially, all glassware and samples were subjected to sterilization by placing them in an autoclave at a temperature of 120 ℃ for a duration of 30 minutes. Both strains were added into a flask containing 100 ml of nutrient broth separately and cultivated for 24 hours in a rotary shaker incubator at 120 rpm. Subsequently, the nutritional agar culture medium was sterilized and added to the individual sterile Petri plates. The antibacterial properties of ZIF-8 and Ag@ZIF-8 were assessed using zone of inhibition tests. This involved using loaded discs (60 µL of 20 mg/mL) of the material with a pore size of 0.2 µm and a diameter of 1 cm, as described by Bharti *et al* (2021). Prior to the placement of the discs, a 100 µL bacterial solution with a concentration of 104 CFU/mL was uniformly distributed

over nutritional agar plates. Following placement on individual plates, the discs loaded with MOF and Ag-MOF nanocomposites (NP-laden discs) and the control disc (which did not contain any nanoparticles) were subjected to a 24-hour incubation period at a temperature of 37 °C. After 24 hours of incubation, the zone of inhibition was measured for each bacterial strain using a ruler. The results were reported as the mean value of ZOI (mm) ± the standard deviation, which were calculated from three repeated measurements.

3. RESULTS AND DISCUSSION

3.1 Synthesis and Characterization

The ZIF-8 and Ag@ZIF-8 materials were successfully synthesized using a simple and environmentally friendly synthesis process. The precursor salts employed were $Zn(NO_3)_2{\cdot}6H_2O$ and $AgNO_3$. The organic ligand employed was H-MIM, while the solvent consisted of a mixture of ethanol and deionized water. Due to its predominant interaction with metal ions, alcohol played a crucial role in the initiation of ZIF formation and the subsequent growth of crystals resulting from the combination of metal and ligand solutions. Water or ethanol was used as a solvent to aid in the creation of a mixture and the dissolving of reactants, which is essential to produce ZIF crystals of superior quality. The other synthesis parameters, such as temperature, pH, stirring power, and reaction time, were kept constant. Following the synthesis, the material was washed using centrifugation. The resulting pellets were then resuspended in ethanol and subsequently in deionized water for further washing. These samples were then employed for characterization and antibacterial investigations. The materials were characterized using UV-Vis spectroscopy to determine their optical properties, FTIR to identify molecular vibrations, XRD to assess the phase development and purity of the synthesized MOFs, and SEM/EDS to analyze the morphology and validate the existence of components in the material.

3.1.1 UV-Vis Spectroscopy

Fig.2 shows the UV-Vis spectra of ZIF-8 and Ag@ZIF-8 samples recorded from 200 to 800 nm. The ZIF-8 and Ag@ZIF-8 samples exhibited identical UV-Vis spectra. ZIF-8 showed a maximum absorption peak at 217 nm. Before taking the absorbance, sonication was done for few minutes for both the samples because ZIF-8 is insoluble in water. In Ag@ZIF-8 absorption peak, some changes were observed due to the presence of Ag in ZIF-8.

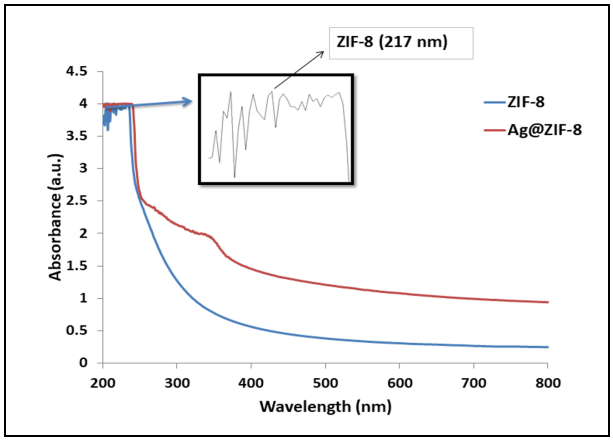


Fig. 2: UV-vis spectra of ZIF-8 and Ag@ZIF-8

3.1.2 XRD Analysis

The crystallinity of the pure ZIF-8 and Ag@ZIF-8 structures was assessed using XRD analysis. The synthesized ZIF-8 pattern (Fig. 3) is consistent with earlier research reported in the literature (Abdi, 2020; Subhadarshini *et al.* 2023). The clearly visible and strong peaks seen at different 2θ values, as shown in Table 1, indicate that ZIF-8 has a sodalite-type structure with excellent crystallinity (Shahsavari *et al.* 2022). The presence of a strong diffraction peak (011) at an angle of 7.2° shows that ZIF-8 has a highly crystalline structure (Du *et al.* 2021). In addition, the diffraction peaks of silver with a face-centered cubic structure may be clearly observed at 2θ = 38° and 44.2° for the (111) and (200) planes, respectively, as reported by Meng *et al.* 2020. Significantly, the introduction of Ag results in a reduction in the intensity of distinct diffraction peaks, indicating the effective integration of Ag ions into the porous structure and surface of ZIF-8.

Table 1. Summary of 2θ value of XRD spectra of ZIF-8 and Ag@ZIF-8 and their corresponding lattice plane

2θ value	Plane	2θ value	Plane
7.29°	011	18.03°	222
10.34°	002	22.12°	114
12.70°	112	24.49°	233
14.67°	022	26.65°	134
16.45°	013		

3.1.3 FTIR analysis

The FTIR analysis was conducted across a range of wavenumbers from 3500 to 600 cm^{-1} to determine the specific bonding groups present in the synthesized MOFs. The prominent bands of the ZIF-8 crystal are linked to the organic ligand H-MIM in the infrared spectrum, as seen in Fig. 4 and outlined in Table 2.

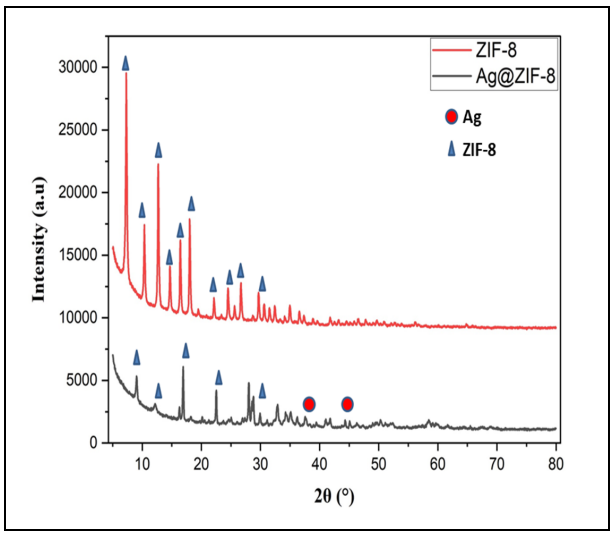


Fig. 3: XRD patterns of ZIF-8 and Ag@ZIF-8

Table 2. FTIR spectra depicting presence of various functional groups of ZIF-8

Frequency Range (cm^{-1})	Functional group
1573	C-N (H-MIM)
2920	C-H bond stretching mode of H-MIM
1428	Stretching vibration of H-MIM
1629	O-H bending vibration
600-1350 and 1350-1500	Bending and stretching vibrations of H-MIM
1144 and 1307	H-MIM bending signals

The characteristic peaks between 600 and 1500 cm^{-1} wavenumbers may be linked to the bending and stretching modes of imidazole rings. Specifically, the range of 600-1350 cm^{-1} corresponds to the bending mode of H-MIM, while the range of 1350-1500 cm^{-1} corresponds to the stretching mode of H-MIM (Abdi, 2020). The distinctive peak at 1428 cm^{-1} reveals the stretching vibration of the imidazole ring (Rahmati et al., 2020). The absorption band at 1573 cm^{-1} is attributed to the stretching vibration of the C=N bond, whilst the peaks at 1144 cm^{-1} and 1307 cm^{-1} correspond to the bending signals of the imidazole ring (Rahmati *et al.* 2020).

The peaks seen at 993 cm^{-1} and 752 cm^{-1} can be ascribed to the bending vibrations of the C-N and C-H bonds, respectively. The O-H bending vibration band is found at 1629 cm^{-1} (Abdi, 2020).

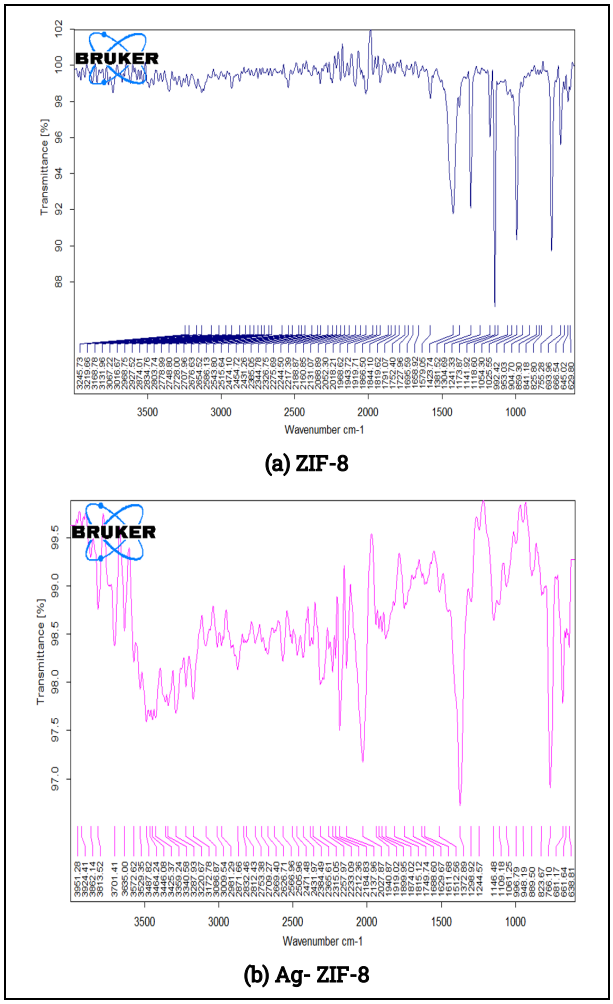


Fig. 4: FTIR spectra of the prepared samples a) ZIF-8 b) Ag@ZIF-8

3.1.4 Morphological Analysis

The morphology of the synthesised materials was studied using SEM as shown in Fig. 5. ZIF-8 particles exemplify non-uniform size because of several conditions on the nucleation process and crystal formation (Fig. 5 a, c, e). The rough surface of Ag@ZIF-8 is a result of the Ag particles being attached to the surface of the ZIF-8 material. Tiny white circles Fig. 5 (b, d, f) provides evidence of the existence of Ag. Additional confirmation of Ag, Zn, C, and O components in ZIF-8 and Ag@ZIF-8 is provided by the elemental studies performed using EDS. The atomic % and weight % of all the elements (Ag, Zn, C, O) are presented in Fig. 6 (b and d).

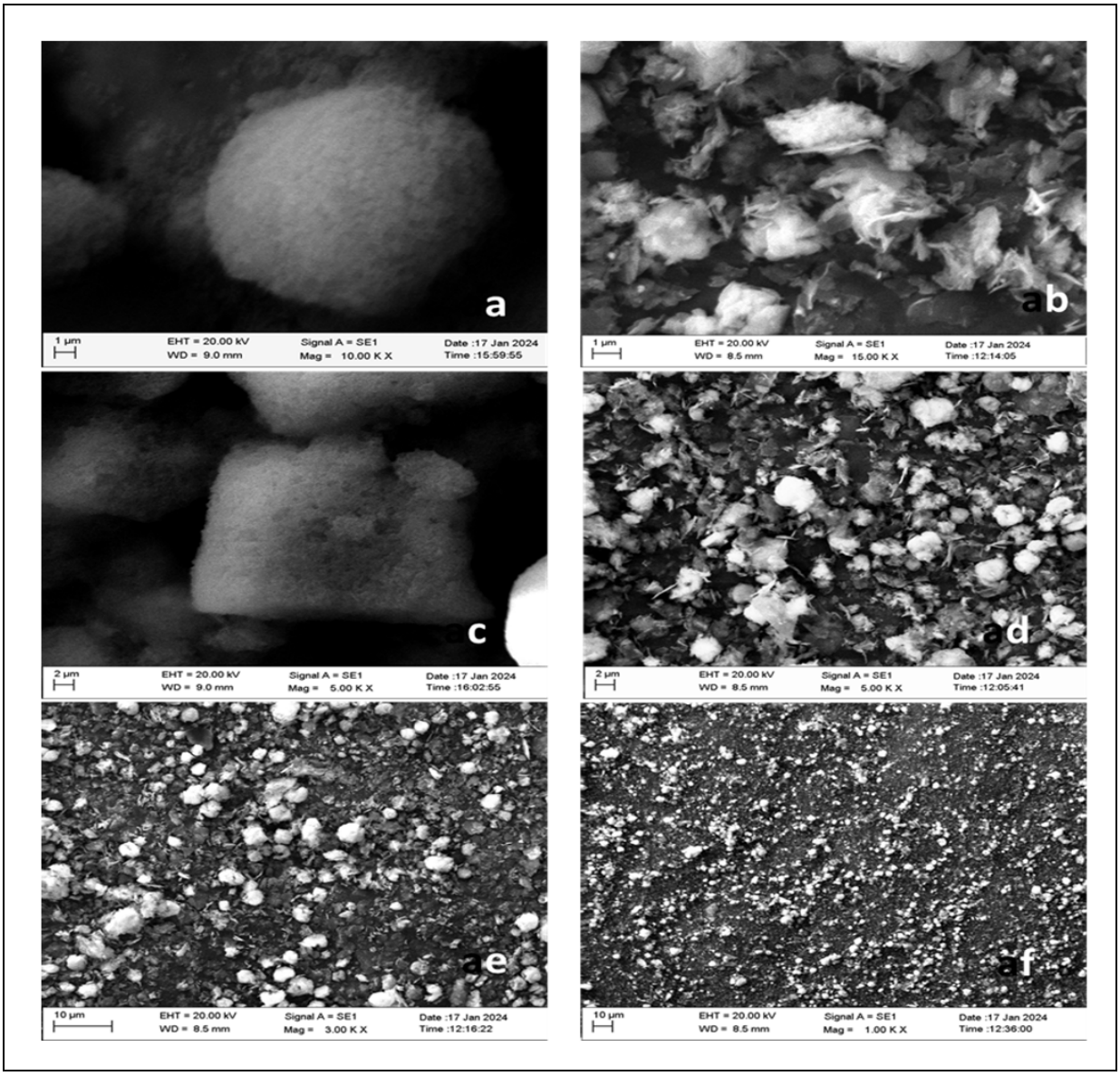
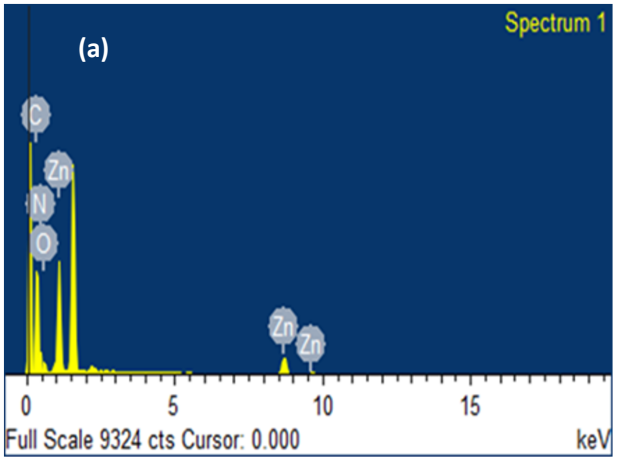
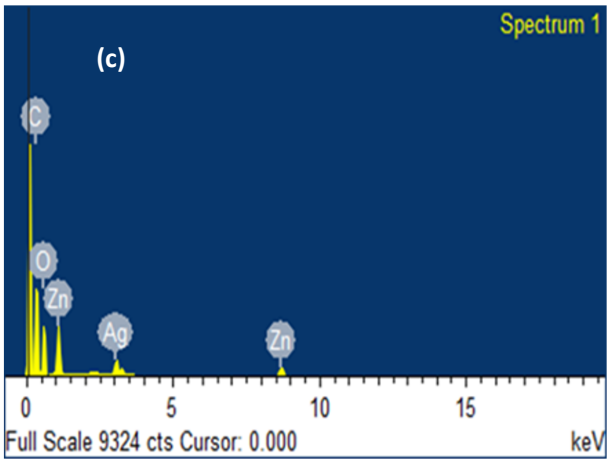


Fig. 5: SEM images of (a, c, e) ZIF-8; (b, d, f) Ag@ZIF-8



(b)

Element	Weight%	Atomic%
C K	11.57	20.16
O K	53.76	70.36
Zn K	21.81	6.98
Ag L	12.86	2.50
Totals	100.00	



(d)

Element	Weight%	Atomic%
C K	11.57	20.16
O K	53.76	70.36
Zn K	21.81	6.98
Ag L	12.86	2.50
Totals	100.00	

Fig. 6: EDS elemental analysis of the ZIF-8 (a and b) and Ag@ZIF-8 (c and d)

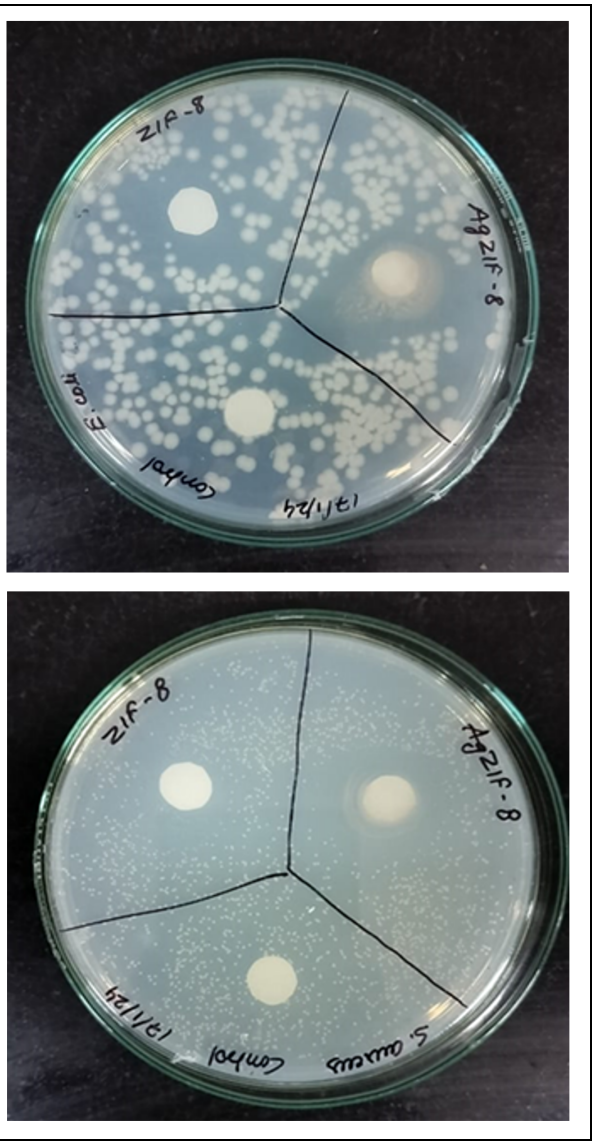


Fig. 7: Inhibition zone of ZIF-8 and Ag@ZIF-8 against *E. coli* and *S. aureus*

Table 3. Previous studies on antibacterial activity using Ag/ZIF-8 composite

Sample	Zone of inhibition (mm)		Reference
	E. coli	*S. aureus*	
Ag@ZIF-8	ZIF-8 = 10 mm; Ag@ZIF-8 = 23 mm	ZIF-8 = 14.8 mm; Ag@ZIF-8 = 25.2 mm	Abdi *et al.* 2020
Ag@ZIF-8	ZIF-8 = no zone; Ag@ZIF-8 = 13 mm	ZIF-8 = no zone Ag@ZIF-8 = 18 mm	Subhadarshini *et al.* 2023
$AgTiO_2$/ ZIF-8	$AgTiO_2$ = 17.6 mm; $AgTiO_2$/ZIF-8 = 22.8 mm	-	Bao *et al.* 2023
ZIF-8/GO/ $MgFe_2O_4$/ TC	TC = 17 mm ZIF-8/GO/ $MgFe_2O_4$ = no zone; ZIF-8/GO/ $MgFe_2O_4$/TC = 22 mm	TC = 18 mm ZIF-8/GO/$MgFe_2$ O4 = no zone; ZIF-8/GO/ $MgFe_2O_4$/TC = 25 mm	Sanaei-Rad *et al.* 2021
Ag@ZIF-8	ZIF-8 = 11.5 mm Ag@ZIF-8 = 29.5 mm	ZIF-8 = 8 mm Ag@ZIF-8 = 21 mm	**This work**

3.2 Disc Diffusion Studies

The antibacterial activity of the synthesised substance was tested by the ZOI assay. The inhibition zone diameters for pure ZIF-8 were 11.5 mm and 8 mm for *E.coli* and *S. aureus*, respectively, while the inhibition zone diameter values for Ag@ZIF-8 were 29.5 mm and 21 mm for *E. coli* and *S. aureus*, respectively (Fig. 7). The results indicate that Ag-doped ZIF-8 has excellent antibacterial properties against both Gram-positive and Gram-negative bacteria. In a separate investigation, ZOI testing was conducted against *E. coli* and *S. aureus*. It was shown that pure ZIF-8 did not exhibit any ZOI against either strain. However, Ag/ZIF-8 demonstrated

ZOI with diameter values of 13 mm and 18 mm against *E. coli* and *S. aureus*, respectively (Subhadarshini *et al.* 2023). Abdi *et al.* (2020) tested the antibacterial properties of Ag@ZIF-8 against two strains. The results showed that the ZOI for pure ZIF-8 was 10 mm and 14.8 mm, respectively. In contrast, Ag@ZIF-8 exhibited ZOI values of 23 mm and 25.2 mm against *E. coli* and *S. aureus*, respectively. Clearly, the nanocomposite exhibited good antibacterial effectiveness compared to both the single pure ZIF-8 and AgNPs (Table 3).

3.3 Antibacterial Mechanism

Based on the experimental results, it is possible to conclude that Ag@ZIF-8 has superior antibacterial activity compared to ZIF-8, as also reported by Rahmati *et al.* (2020). The following was suggested as potential antibacterial mechanisms of AgNPs, ZIF-8, and Ag@ZIF-8. Higher ZOI in the case of Ag@ZIF-8 may be attributed to AgNPs and released silver ions, causing inhibition of bacterial growth (Rahmati *et al.* 2020). Various mechanisms have been documented regarding the antibacterial agent role of AgNPs, as illustrated in Fig. 8. Due to the affinity for sulphur-containing proteins of Ag, which can damage or alter the structures of strains, AgNPs can adhere to the cell membranes of bacteria (Thakur *et al.* 2023). By complexing with RNA and DNA, AgNPs can condense and prevent DNA replication. This binding of AgNPs with thiol groups in proteins deactivates the function of respiratory enzymes (Bharti *et al.* 2021). Furthermore, the interactions between Ag^{+} and the structure of DNA can inhibit bacterial growth. As a result, the bacterial cell growth is inhibited, the cell membrane gets ruptured, leading to cell death as the outer layer loses its protection. AgNPs cause oxidative stress in cells by producing reactive oxygen species (ROS), damaging proteins and nucleic acids, and ultimately stopping cells from proliferating (Bharti *et al.* 2020; Bharti *et al.* 2023a). Furthermore, when Ag@ZIF-8 is added to bacterial solution, it can release Zn^{2+} and Ag^{+} with less toxicity and biological antibacterial activity. These metal ions come into close contact with bacteria, where they can attach themselves to the component proteins in their cell walls and membranes, denaturing and deactivating them (Cao *et al.* 2020; Yan *et al.* 2022). The inherent antibacterial characteristic of metal ions liberated from zinc ions is thought to be the cause of the antimicrobial effect of ZIF-8. Because ZIF-8 has a porous structure and a high BET surface area, more Ag is equally spread on its surface. This increases the area of contact between the bacteria and the bactericidal agent, enhancing the antibacterial activity. Furthermore, Ag@ZIF-8 can be gradually released to release Ag^{+} and Zn^{2+}, thereby providing a sustained antibacterial action (Yan *et al.* 2022). In conclusion, Ag@ZIF-8's strong antibacterial activity results from its synergistic actions.

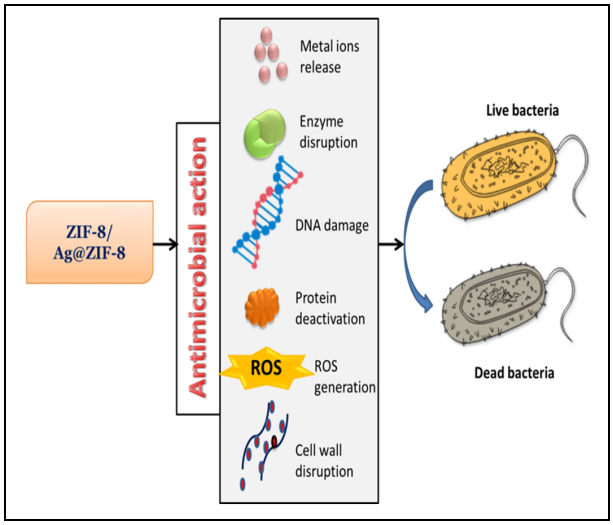


Fig. 8: Possible mode of antimicrobial action of ZIF-8/ Ag@ZIF-8

4. CONCLUSION

The MOFs, ZIF-8 and Ag@ZIF-8 were successfully produced using a basic green synthesis process at room temperature. The effective synthesis of these materials was proven using various characterization techniques such as, UV-Vis spectrophotometry, FTIR, XRD, and SEM/EDS. To examine the antibacterial activity of ZIF-8 and Ag@ZIF-8, zone of inhibition tests against Gram-positive (*S. aureus* MTCC 9542) and Gram-negative (*E. coli*) bacteria were conducted. Pure ZIF-8 suppressed the growth of *S. aureus* and *E. coli* with inhibition zone sizes of 11.5 mm and 8 mm, respectively. In comparison, Ag@ZIF-8 displayed inhibitory zone diameters of 29.5 mm and 21 mm for *S. aureus* and *E. coli*, respectively. The results suggest that Ag@ZIF-8 exhibits enhanced antibacterial efficacy compared to pure ZIF-8 against both pathogens. Findings collectively highlight the promising potential of silver nanoparticles, various ZIFs, and their synergistic effects as avenues for developing novel antimicrobial medicines. Further investigations into these nanomaterials and their interactions may unlock new strategies for combating bacterial infections and addressing antimicrobial resistance, while reducing adverse effects.

FUNDING

This research received no specific grant from any funding agency in the public, commercial, or not-for-profit sectors.

CONFLICTS OF INTEREST

The authors declare that there is no conflict of interest.

CREDIT AUTHOR STATEMENT

Suman Thakur: Writing- Conducted experiments, Data analysis, original draft preparation. Sharda Bharti: Conceptualization, Data analysis, Reviewing and Editing, Visualization, Supervision.

ACKNOWLEDGEMENTS

The authors would like to acknowledge the National Institute of Technology (NIT) Raipur for offering the necessary facilities to carry out this work, for partial funding support through Seed Grant Project (NITRR/Dean(R&C)/2022/85), and all other support in completing this manuscript.

COPYRIGHT

This article is an open-access article distributed under the terms and conditions of the Creative Commons Attribution (CC BY) license (http://creativecommons.org/licenses/by/4.0/).



REFERENCES

Abdi, J., Synthesis of Ag-doped ZIF-8 photocatalyst with excellent performance for dye degradation and antibacterial activity, *Colloids Surfaces A Physicochem. Eng. Asp.* 604, 125330 (2020). https://doi.org/10.1016/j.colsurfa.2020.125330

Amargeetha, A. and Velavan, S., X-ray Diffraction (XRD) and Energy Dispersive Spectroscopy (EDS) Analysis of Silver Nanoparticles Synthesized from Erythrina Indica Flowers, *Nanosci. Technol. Open Access* 5(1), 1–5 (2018). https://doi.org/10.15226/2374-8141/5/1/00152

Bao, S., Sun, S., Li, L. and Xu, L., Synthesis and antibacterial activities of Ag-TiO2/ZIF-8, Front Bioeng Biotechnol. https://doi.org/10.3389/fbioe.2023.1221458

Bergaoui, M., Khalfaoui, M., Awadallah-F, A. and Al-Muhtaseb, S., A review of the features and applications of ZIF-8 and its derivatives for separating CO2 and isomers of C3- and C4-hydrocarbons, *J. Nat. Gas Sci. Eng.* 96, 104289 (2021). https://doi.org/10.1016/j.jngse.2021.104289

Bharti, S., Anant, P. S. and Kumar, A., Nanotechnology in stem cell research and therapy, *J. Nanoparticle Res.* 25(1), 6 (2023a). https://doi.org/10.1007/s11051-022-05654-6

Bharti, S. and Kumar, A., Synergies in stem cell research: Integrating technologies, strategies, and bionanomaterial innovations, *Acta Histochem.* 126(1), 152119 (2024). https://doi.org/10.1016/j.acthis.2023.152119

Bharti, S., Mukherji, S. and Mukherji, S., Extracellular synthesis of silver nanoparticles by Thiosphaera pantotropha and evaluation of their antibacterial and cytotoxic effects, *3 Biotech* 10(6), 237 (2020). https://doi.org/10.1007/s13205-020-02218-0

Bharti, S., Mukherji, S. and Mukherji, S., Water disinfection using fixed bed reactors packed with silver nanoparticle immobilized glass capillary tubes, *Sci. Total Environ.* 689, 991–1000 (2019). https://doi.org/10.1016/j.scitotenv.2019.06.482

Bharti, S., Mukherji, S. and Mukherji, S., Enhanced antibacterial activity of decahedral silver nanoparticles, *J. Nanoparticle Res.* 23(2), 36 (2021). https://doi.org/10.1007/s11051-020-05106-z

Bharti, S., Nag, P., Sadani, K., Mukherji, S. and Mukherji, S., Exploring the Application, Safety, and Challenges of Free Versus Immobilized Antimicrobial Nanomaterials, In: Applications of Nanotechnology in Microbiology. Springer Nature Switzerland, Cham, pp 97–133 (2023). https://doi.org/10.1007/978-3-031-49933-3_5

Cao, P., Wu, X., Zhang, W., Zhao, L., Sun, W. and Tang, Z., Killing Oral Bacteria Using Metal-Organic Frameworks, *Ind. Eng. Chem. Res.* 59(4), 1559–1567 (2020). https://doi.org/10.1021/acs.iecr.9b05659

Du, P. D., Hieu, N. T. and Thien, T. V., Ultrasound-Assisted Rapid ZIF-8 Synthesis, Porous ZnO Preparation by Heating ZIF-8, and Their Photocatalytic Activity, *J. Nanomater.,* 2021, 1–12 (2021). https://doi.org/10.1155/2021/9988998

Franci, G., Falanga, A., Galdiero, S., Palomba, L., Rai, M., Morelli, G. and Galdiero, M., Silver Nanoparticles as Potential Antibacterial Agents, *Mol.,* 20(5), 8856–8874 (2015). https://doi.org/10.3390/molecules20058856

Gu, A., Chen, J., Gao, Q., Khan, M. M., Wang, P., Jiao, Y., Zhang, Z., Liu, Y. and Yang, Y., The preparation of Ag/ZIF-8@ZIF-67 core-shell composites as excellent catalyst for degradation of the nitroaromatic compounds, *Appl. Surf. Sci.,* 516, 146160 (2020). https://doi.org/10.1016/j.apsusc.2020.146160

Guo, Y.-F., Fang, W.-J., Fu, J.-R., Wu, Y., Zheng, J., Gao, G.-Q., Chen, C., Yan, R.-W., Huang, S.-G. and Wang, C.-C., Facile synthesis of Ag@ZIF-8 core-shell heterostructure nanowires for improved antibacterial activities, *Appl. Surf. Sci.,* 435, 149–155 (2018). https://doi.org/10.1016/j.apsusc.2017.11.096

Kumar, P., Gacem, A., Ahmad, M. T., Yadav, V. K., Singh, S., Yadav, K. K., Alam, M. M., Dawane, V., Piplode, S., Maurya, P., Ahn, Y., Jeon, B. H. and Cabral-Pinto, M. M. S., Environmental and human health implications of metal(loid)s: Source identification, contamination, toxicity, and sustainable clean-up technologies, *Front. Environ. Sci.* 10(August), 1–23 (2022). https://doi.org/10.3389/fenvs.2022.949581

Malik, A., Nath, M., Mohiyuddin, S. and Packirisamy, G., Multifunctional CdSNPs@ZIF-8: Potential Antibacterial Agent against GFP-Expressing Escherichia coli and Staphylococcus aureus and Efficient Photocatalyst for Degradation of Methylene Blue, *ACS Omega* 3(7), 8288–8308 (2018). https://doi.org/10.1021/acsomega.8b00664

Meng, X., Duan, C., Zhang, Y., Lu, W., Wang, W. and Ni, Y., Corncob-supported Ag NPs@ ZIF-8 nanohybrids as multifunction biosorbents for wastewater remediation: Robust adsorption, catalysis and antibacterial activity, *Compos. Sci. Technol.* 200, 108384 (2020). https://doi.org/10.1016/j.compscitech.2020.108384

Rahmati, Z., Abdi, J., Vossoughi, M. and Alemzadeh, I., Ag-doped magnetic metal organic framework as a novel nanostructured material for highly efficient antibacterial activity, *Environ. Res.* 188, 109555 (2020). https://doi.org/10.1016/j.envres.2020.109555

Salehipour, M., Rezaei, S., Rezaei, M., Yazdani, M. and Mogharabi-Manzari, M., Opportunities and Challenges in Biomedical Applications of Metal–Organic Frameworks, *J. Inorg. Organomet. Polym. Mater.* 31(12), 4443–4462 (2021). https://doi.org/10.1007/s10904-021-02118-7

Sanaei-Rad, S., Ghasemzadeh, M. A. and Razavian, S. M. H., Synthesis of a novel ternary ZIF-8/GO/MgFe2O4 nanocomposite and its application in drug delivery, *Sci. Rep.* 11(1), 18734 (2021). https://doi.org/10.1038/s41598-021-98133-2

Shahsavari, M., Jahani, P. M., Sheikhshoaie, I., Tajik, S., Afshar, A. A., Askari, M. B., Salarizadeh, P., Di Bartolomeo, A. and Beitollahi, H., Green Synthesis of Zeolitic Imidazolate Frameworks: A Review of Their Characterization and Industrial and Medical Applications, *Materials (Basel).* 15(2), 1–27 (2022). https://doi.org/10.3390/ma15020447

Subhadarshini, A., Samal, S. K., Pattnaik, A. and Nanda, B., Facile fabrication of plasmonic Ag/ZIF-8: an efficient catalyst for investigation of antibacterial, haemolytic and photocatalytic degradation of antibiotics, *RSC Adv.* 13(45), 31756–31771 (2023). https://doi.org/10.1039/D3RA04851A

Thakur, S. and Bharti, S., The synergy of nanoparticles and metal-organic frameworks in antimicrobial applications: A critical review, *J. Environ. Chem. Eng.* 11(6), 111458 (2023). https://doi.org/10.1016/j.jece.2023.111458

Yan, L., Gopal, A., Kashif, S., Hazelton, P., Lan, M., Zhang, W. and Chen, X., Metal organic frameworks for antibacterial applications, *Chem. Eng. J.* 435(P2), 134975 (2022). https://doi.org/10.1016/j.cej.2022.134975

Yuan, J., Li, Q., Shen, J., Huang, K., Liu, G., Zhao, J., Duan, J. and Jin, W., Hydrophobic-functionalized ZIF-8 nanoparticles incorporated PDMS membranes for high-selective separation of propane/nitrogen, *Asia-Pacific J. Chem. Eng.* 12(1), 110–120 (2017). https://doi.org/10.1002/apj.2058